A Water Stable and Highly Fluorescent Zn(II) Based Metal−Organic Frameworks for Fast Detection of Hg^{2+}, Cr^{VI} and Antibiotics

Chaoxiong Li,[a] Xuancheng Sun,[a] Xianggao Meng,*[b] Dunjia Wang[a] and Chunyang Zheng*[a]

[a] Hubei Key Laboratory of Pollutant Analysis and Reuse Technology, Institute for Advanced Materials, Hubei Normal University, Huangshi 435002, P. R. China.

[b] College of Chemistry, Central China Normal University, Wuhan 430079, P. R. China.

* E-mail: mengxianggao@ccnu.edu.cn; cyzheng@hbnu.edu.cn

CONTENTS

Materials and methods

With the exception of BBDF, all solvents and materials were purchased without any purification. Powder X-ray diffraction (XRD) were performed on Bruker D2 PHASER diffractometer with Cu-$K\alpha$ radiation (λ= 1.54186 Å). Thermogravimetric analysis was carried out with a NETZSCH STA 449F5 (TG/DTA) thermal analyzer under nitrogen flow. IR spectra of the two compounds were performed on a Bruker AXS TENSOR-27 FT-IR spectrometer (FTIR) with pressed KBr pellets in the range of 4000–400 cm^{-1}. Fluorescence measurements were carried out on an F4700 (Hitachi) fluorescence spectrophotometer at room temperature. UV-vis absorption analysis was performed on a U-3010 spectrophotometer at room temperature.

Crystallographic studies

Single-crystal X-ray diffraction data of **1** were collected on a Bruker APEX-II CCD with ω-scan pattern and Ga-Kα radiation (λ = 1.34139 Å) at 200 K. The structures were solved with direct methods (SHELX), and refined by fullmatrix least squares on F^2 using OLEX3, which utilizes the SHELXL-2018 module. The hydrogen atoms were placed geometrically. All non-hydrogen atoms were refined anisotropically. The H atoms of ATP^{2-} and BBDF were generated from the computed positions and subjected to isotropic refinement. The guest DMF molecules and water molecules are too disordered to be modeled properly. So the diffuse electron densities resulting from these solvent molecules are removed by using the SQUEEZE routine of PLATON program to produce solvent-free diffraction intensities. The guest molecules were quantified through the elemental analyses and thermogravimetric analyses. The relevant crystallographic data are summarized in Table 1. The chosen bond lengths as well as angles are presented in Table S2.

Fluorescence Measurements

Luminescent spectra were recorded with a F4700 (Hitachi) fluorescence spectrophotometer at room temperature. The cation incorporated **1** emulsions were prepared by introducing 3 mg of **1** powder into 3.00 mL of aqueous solution containing K^+, Na^+, Zn^{2+}, Cd^{2+}, Mn^{2+}, Hg^{2+}, Ag^+, Co^{2+}, Ni^{2+}, Mg^{2+}, Cu^{2+}, Pb^{2+}, Al^{3+} and Cr^{3+} at a concentration of 0.1 mM. For sensing properties with respect to Hg^{2+}, 3 mg of 1 powder was dispersed in 3.00 mL of Hg^{2+} aqueous solution with different concentrations. The anions incorporated **1** emulsions were prepared by introducing 3 mg of 1 powder into 3.00 mL of sodium salts aqueous solution of NO_2^-, Br^-, I^-, Cl^-, $H_2PO_4^-$, SO_4^{2-}, NO_3^-, WO_4^{2-}, Ac^-, SCN^-, HPO_4^{2-}, HCO_3^-, CO_3^{2-}, $Cr_2O_7^{2-}$ and CrO_4^{2-} at a concentration of 0.5 mM. For sensing properties with respect to $Cr_2O_7^{2-}$, 3 mg of 1 powder was added into 3.00 mL of $Cr_2O_7^2$ aqueous solution with different concentrations.

The antibiotics incorporated **1** emulsions were prepared by introducing 3 mg of **1** powder into 3.00 mL of sodium salts aqueous solution of NFZ, NFT, ODZ, RDZ, MDZ, DTZ, SMZ, SDZ, STZ, CAP, CPF and LOF at a concentration of 0.2 mM. For sensing properties with respect to

$Cr_2O_7^{2-}$, 3 mg of **1** powder was added into 3.00 mL of NFZ or NFT aqueous solution with different concentrations. The finely ground powder of complex **1** is dispersed well in the solution, which enables substrates to be closely adhered to the surface of the MOF particles and facilitates possible host–guest interactions. To obtain the luminescent spectra, the emulsions were treated by ultrasonic treatment for 30 min to form stable emulsions before fluorescence study. Each PL emission spectra were measured at least three times and the emission intensities were found basically unvaried.

Synthesis of BBDF

A flame-dried Schlenk flask was charged with A mixture of 2,7-dibromo-9,9-dimethyl-9*H*-fluorene (3.52 g, 10 mmol), benzimidazole (5.90 g, 50 mmol),, K_2CO_3 (10.00 g, 72 mmol), CuI (0.44 g, 2.3 mmol) and DMF(100 mL) at room temperature under nitrogen. After being heated at 120 ºC for 72 h, the mixture was evaporated under vacuum. Thereafter, 100 mL of distilled water was added to facilitate the workup. The mixture was extracted three times with CH_2Cl_2 (100 mL), then the organic phase was further washed with distilled water and dried with anhydrous $MgSO_4$. After the filtration and evaporation, the resulting residue was purified by flash column chromatography on silica gel eluting with CH_2Cl_2/MeOH (20: 1) to give BBDF as a pale-yellow solid. Isolated yield: 2.3 g (54%). ^{1}H NMR (300 MHz, $CDCl_3$): δ 1.64 (s, 6H), 7.38 (d *J* = 5.1 Hz, 5H), 7.55-7.62 (m, 6H), 7.97 (d *J* = 8.1 Hz,4H), 8.28 (s, 2H) ppm; ^{13}C NMR (75.4 MHz, $CDCl_3$): δ 27.1, 47.7, 110.6, 118.7, 120.8, 121.7, 122.9, 123.4, 135.9, 137.9, 155.8 ppm. Yellow block crystals of BBDF were obtained by recrystallization in the mixed solvent of DMF and H_2O. The detailed crystal data and structure refinement parameters are shown in Table 1.

Table S1 Selected bond lengths (Å) and angles (°) for **1**

Zn1-O1	2.1434(15)	Zn1-O2	2.2647(18)
Zn1-O3#1	2.176(2)	Zn1-O4#1	2.254(2)
Zn1-N2	2.0430(16)	Zn1-N5#2	2.0721(16)
O1-Zn1-O2	59.57(6)	O1-Zn1-O3#1	101.54(7)
O1-Zn1-O4#1	150.36(8)	O3-Zn1-O2#1	89.26(7)
O3#1-Zn1-O4#1	58.58(8)	N2-Zn1-O1	106.48(6)
O4-Zn1-O2	96.00(7)	N2-Zn1-O2	94.34(6)
N5-Zn1-O1#2	93.29(6)	N2-Zn1-O3#1	149.37(8)
N5-Zn1-O2#2	152.38(6)	N2-Zn1-O4#1	90.80(7)
N5#2-Zn1-O3#1	91.66(7)	N2-Zn1-N5#2	98.74(7)
N5#2-Zn1-O4#1	107.97(7)		
Symmetry codes: #1: x, 1-y, -1/2+z #2: -1+x, y, z			

Table S2 SHAPE analysis of the Zn^{II} ions in **1**.

ions	label	shape	symmetry	distortion(τ)
	HP-6	Hexagon	D_{6h}	32.122
	PPY-6	Pentagonal pyramid	C_{5v}	19.092
Zn1	OC-6	Octahedron	O_h	**5.715**
	TPR-6	Trigonal prism	D_{3h}	10.611
	JPPY-6	Johnson pentagonal pyramid J2	C_{5v}	23.320

Table S3 Comparison of **1** with recent MOF-based luminescent sensors for Hg^{2+}.

MOF-based chemosensor	Analyst	$K_{sv} \times 10^4$ /M^{-1}	LOD	Medium	Ref.
$[Zn(\mu_2\text{-}1H\text{-ade})(\mu_2\text{-}SO_4)]_n$	Hg^{2+}	0.77	0.07 μM	H_2O	1
$[Zn_2(bbmb)_2(tdc)_2] \cdot 2H_2O$	Hg^{2+}	48.1	0.19 μM	H_2O	2
$Cd_3(C_{10}H_4O_7N_1)_2(H_2O)_8]$ $0.733(O_2) \cdot 2(H_{1.47} O_{0.27})$	Hg^{2+}	11.4	5.4 ppb	H_2O	3
$\{[Cd_{1.5}(C_{18}H_{10}O_{10})] \cdot (H_3O)(H_2O)_3\}n$	Hg^{2+}	0.43	NR	H_2O	4
$Eu^{3+}@UIO\text{-}66(DPA)$	Hg^{2+}	137	8.26 nM	H_2O	5
$[Zn(2\text{-}NH_2bdc)(bibp)]n$	Hg^{2+}	655	4.2×10^{-8} M	H_2O	6
$\{[Cd(BIBT)(TDC)] \cdot 2H_2O\}n$	Hg^{2+}	5.05	0.097 μM	H_2O	7
$[Zr_6O_4(OH)_4(C_{12}H_4S_2)_{4.9}] \cdot 4H_2O \cdot 4DMF$	Hg^{2+}	35.4	5 nM	H_2O	8
$[Zn_3(ssa)_2(1,4\text{-}bib)_3 \cdot 4H_2O]n$	Hg^{2+}	19.8	0.23 μM	H_2O	9
$[Cd(L)(NTA)]n$	Hg^{2+}	0.357	3.05 μM	H_2O	10
$[Ni(L)(NPTA) H_2O]n$		0.743	2.29 μM		
$\{[Cd(BIPA)(tfbdc)(H_2O)] \cdot DMF\}n$	Hg^{2+}	1.27	0.12 μM	H_2O	11
$[Co(NPDC)(bpee)] \cdot DMF \cdot 2H_2O$	Hg^{2+}	0.426	4.1 μM	H_2O	12
$\{[Zn(BBDF)(ATP)] \cdot 2DMF \cdot 3H_2O\}_n$	**Hg^{2+}**	**3.89**	**0.12 μM**	H_2O	**this work**

Table S4 Comparison of **1** with recent MOF-based luminescent sensors for $Cr_2O_7^{2-}$ and CrO_4^{2-}
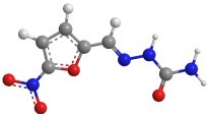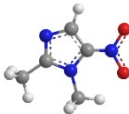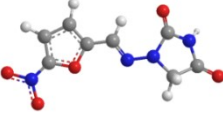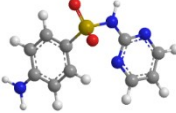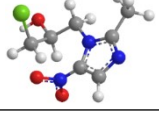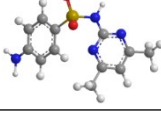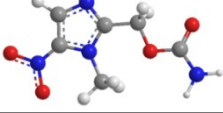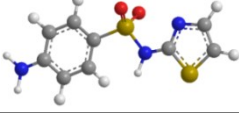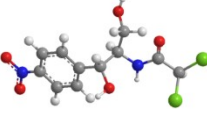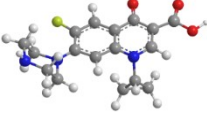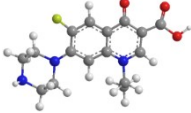
MOF-based chemosensor	Analyst	$K_{SV} \times 10^4$ /M^{-1}	LOD	Medium	Ref.
Zn-(PBBA)(H$_2$O)]·3DMF·2H$_2$O	$Cr_2O_7^{2-}$	1.2	4.2 μM	H$_2$O	13
{[Zn(L)$_{0.5}$(bpea)]·0.5H$_2$O·0.5DMF	$Cr_2O_7^{2-}$	1.65	1.42 μM	H$_2$O	14
	CrO_4^{2-}	1.34	2.65 μM		
{[Zn-(L)$_{0.5}$(ibpt)]·H$_2$O·DMF}$_n$	$Cr_2O_7^{2-}$	1.02	2.21 μM		
	CrO_4^{2-}	1.26	3.78μM		
[Zn(L1)hfdba]n	$Cr_2O_7^{2}$	0.5029	0.33 μM	H$_2$O	15
	CrO_4^{2-}	0.22387	0.745 μM		
{[Zn(L$_2$)(hfdba)$_2$]·2H$_2$O}n.	$Cr_2O_7^{2}$	1.3268	83.5 μM		
	CrO_4^{2-}	0.9079	114.2 μM		
Gd$_{10}$L$_6$(OH)$_4$(H$_2$O)$_3$]·4C$_2$H$_8$N	$Cr_2O_7^{2-}$	NR	2.68 μM	H$_2$O	16
{[Cd(μ_5-L) I}n	$Cr_2O_7^{2-}$	1.85	NR	H$_2$O	17
[Zn(OBA)$_2$(L$_1$)·2DMA]$_n$	$Cr_2O_7^{2-}$	1.897	2.37μM	H$_2$O	18
	CrO_4^{2-}	1.1605	3.87 μM		
[Zn(ttb)(bdc)$_{0.5}$]$_n$	$Cr_2O_7^{2-}$	6.67	0.10 μM	H$_2$O	19
Cd$_3$L(BTB)$_2$·2DMF	$Cr_2O_7^{2-}$	2.06	1.2 μM	H$_2$O	20
(Cd$_3$O$_2$)LBTC		2.44	1.4 μM		
[Zn(L)·2MeOH·H$_2$O]	$Cr_2O_7^{2-}$	0.118	2.95 μM	H$_2$O	21
[Cd$_{1.5}$(L)$_2$(bpy)(NO$_3$)]·2DMF·2H$_2$O	$Cr_2O_7^{2-}$	5.42	320 ppb	H$_2$O	22
	CrO_4^{2-}	1.73	320 ppb		
Zn$_2$(tpeb)(bpdc)$_2$·0.5DMA·4H$_2$O	$Cr_2O_7^{2-}$	1.122	1.04 μM	H$_2$O	23
	CrO_4^{2-}	1.085	1.07 μM		
{[Zn$_3$(mtrb)$_3$(btc)$_2$]·3H$_2$O}n	$Cr_2O_7^{2-}$	0.277	4.52 M	H$_2$O	24
{[Zn(BBDF)(ATP)]·2DMF·3H$_2$O}$_n$	**$Cr_2O_7^{2-}$**	**2.64**	**0.17 μM**	H$_2$O	**this work**

Table S5 Comparison of **1** with recent MOF-based luminescent sensors for NFZ and NFT

MOF-based chemosensor	Analyst	$K_{SV}\times10^4$ /M^{-1}	LOD	Medium	Ref.
{[Eu$_2$Na(Hpdbb)(pdbb)$_2$ (CH$_3$COO)$_2$]·2.5DMA}$_n$	NFZ	4.85	0.64 μM	DMF	25
	NFT	4.39	0.68 μM		
[Cd$_2$(L$_2$)(bpda)$_2$]·3DMF·H$_2$O	NFZ	3.1	1.27 μM	DMF	26
	NFT	2.2	1.95 μM		
{[Eu(H$_2$O)(BTCTB)]·2H$_2$O}n	NFZ	1.27	0.67 μM	H$_2$O	27
	NFT	2.1	0.6 μM		
[Eu(cppa)(OH)]·xS	NFT	2.33	0.43 μM	H$_2$O	28
Zr$_6$O$_4$(OH)$_8$(H$_2$O)$_4$(CTTA)$_{8/3}$	NFZ	11	NR	H$_2$O	29
	NFT	3.8	NR		
Zr$_6$O$_4$(OH)$_8$(H$_2$O)$_4$(TTNA)$_{8/3}$	NFZ	7.5	NR		
	NFT	6.0	NR		
[Zn(C$_{18}$N$_2$O$_4$H$_{10}$)H$_2$O]·DMF	NFT	6.0	0.14 μM	Ethanol	30
	NFZ	4.73	0.19 μM		
Cd$_3$·L·(BTB)$_2$·2DMF	NFT	6.81	0.44 μM	DMF	31
Cd$_3$O$_2$)·L·BTC		3.80	0.78 μM		
{[Zn$_2$(TRZ)$_2$(DBTDC-O$_2$)]·DMAc}$_n$	NFZ	4.5	0.404 μM	H$_2$O	32
	NFT	18	0.353 μM		
{[Cd$_2$(Py$_2$TTz)$_2$(BDC)$_2$]·2(DMF)}$_n$	NFZ	4.4	0.85 μM	H$_2$O	33
[Cd$_3$(CBCD)$_2$(DMA)$_4$(H$_2$O)$_2$]·10DMA	NFT	9.72	85 ppb	DMA	34
	NFT	6.39	128 ppb		
RhB@ZIF-8	NFZ	7.3	0.26 μM	H$_2$O	35
	NFT	1.8	0.47μM		
[Zn$_3$(bpg)$_{1.5}$(azdc)$_3$]·(DMF)$_{5.9}$·(H$_2$O)$_{1.05}$	NFZ	8.75	0.66 μM	DMF	36
	NFT	5.92	NR		
{[(CH$_3$)$_2$NH$_2$]$_2$[Pb(TCBPE)(H$_2$O)$_2$]}$_n$	NFZ	1.934	0.35 μM	H$_2$O	37
	NFT	2.01	0.33 μM		
[In(dtztp)$_{0.5}$(OH)(H$_2$O)]·H$_2$O	NFT	6.26	7.4 ppm	H$_2$O	38
[Mg$_2$(APDA)$_2$(H$_2$O)$_3$]·5DMA·5H$_2$O	NFZ	9.0	108 ppb	DMF	39
	NFT	8.82	126 ppb		
[In$_2$(L)(OH)$_2$]·2DMF·2H$_2$O	NFZ	3.35	0.55 μM	DMF	40
[(CH$_3$)$_2$NH$_2$][TbZn$_3$(L)$_3$(HCOO)(H$_2$O)$_2$·5H$_2$O	NFT	183	39 ppb	H$_2$O	41
	NFZ	92.5	52 ppb		
{[Zn(BBDF)(ATP)]·2DMF·3H$_2$O}$_n$	NFT	4.65	0.098 μM	H$_2$O	**this work**
	NFZ	3.95	0.14 μM		

Note. NR: Not report

Table S6 Structure of 12 antibiotics

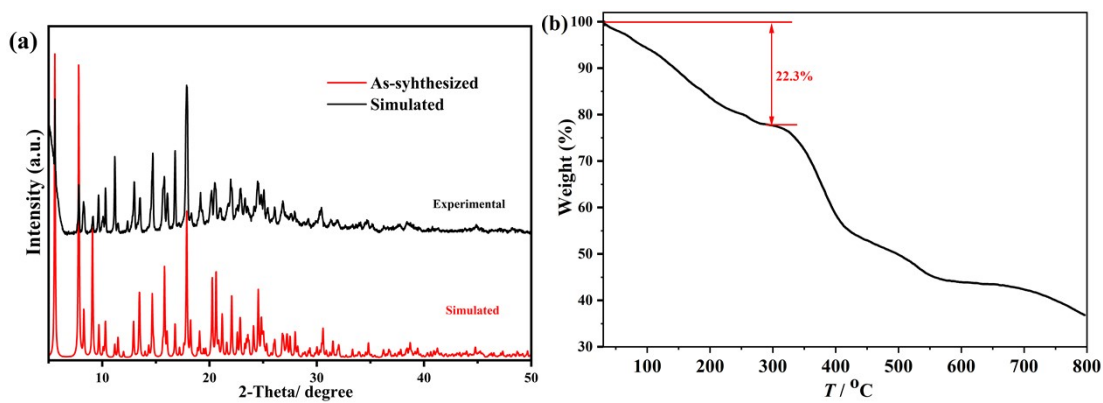| Name	Structure	Name	Structure
Nitrofurazone **NFZ**		Dimetridazole **DTZ**	
Nitrofurantoin **NFT**		Sulfadiazine **SDZ**	
Ornidazole **ODZ**		Sulfamethazine **SMZ**	
Ronidazole **RDZ**		Sulfathiazole **STZ**	
Metronidazole **MDZ**		Chloramphenicol **CAP**	
Ciprofloxacin **CPF**		Norfloxacin **NOF**	

Fig. S1 (a) The simulated and experimental PXRD patterns of **1**; (b) The TGA curve for **1** under N$_2$ atmosphere
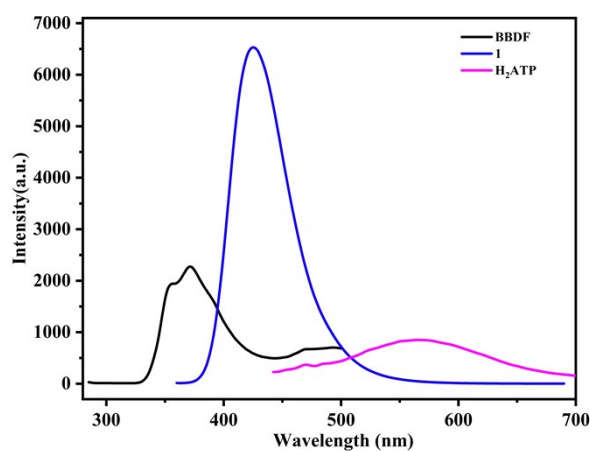

Fig. S2 Fluorescent emission spectra of free ligand BBDF and H$_2$ATP, as well as compound **1** in solid state at room temperature.
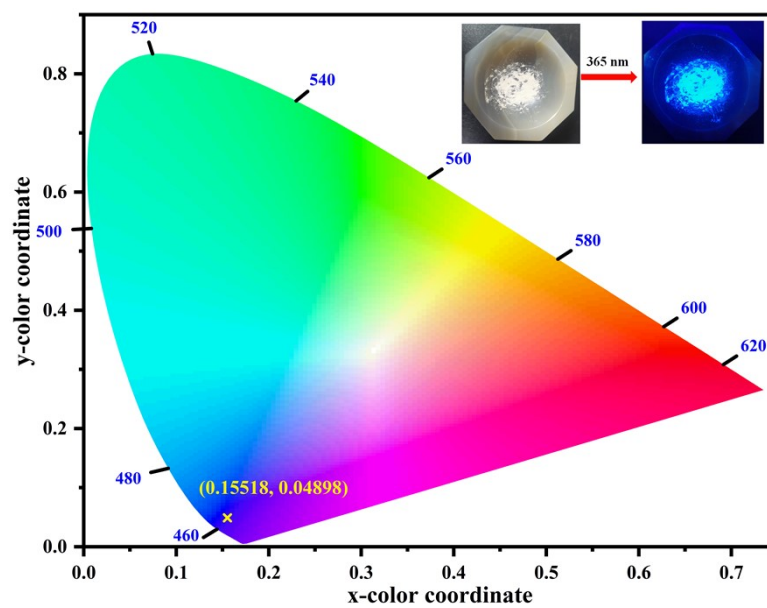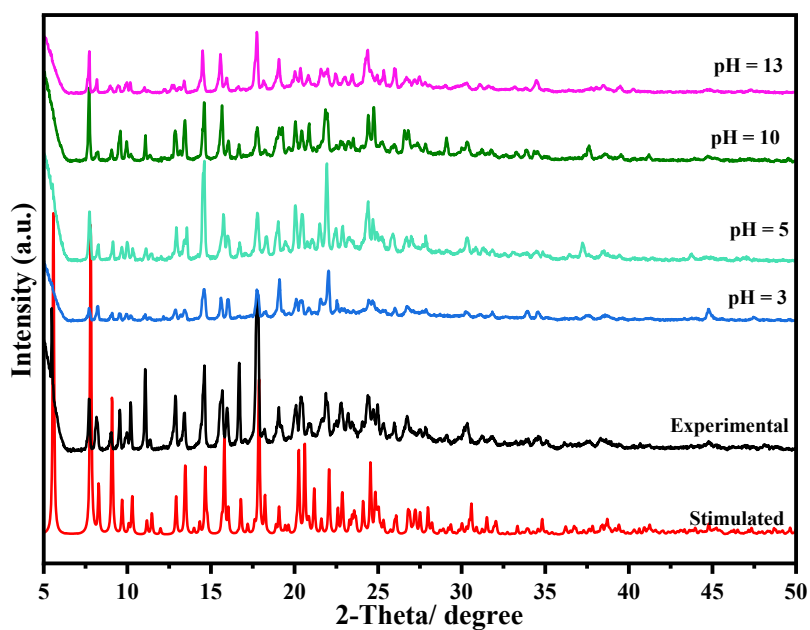

Figure S3 CIE coordinates of **1**

Fig. S4 The simulated and experimental PXRD patterns of **1** after immersing in aqueous solution with diverse pH values
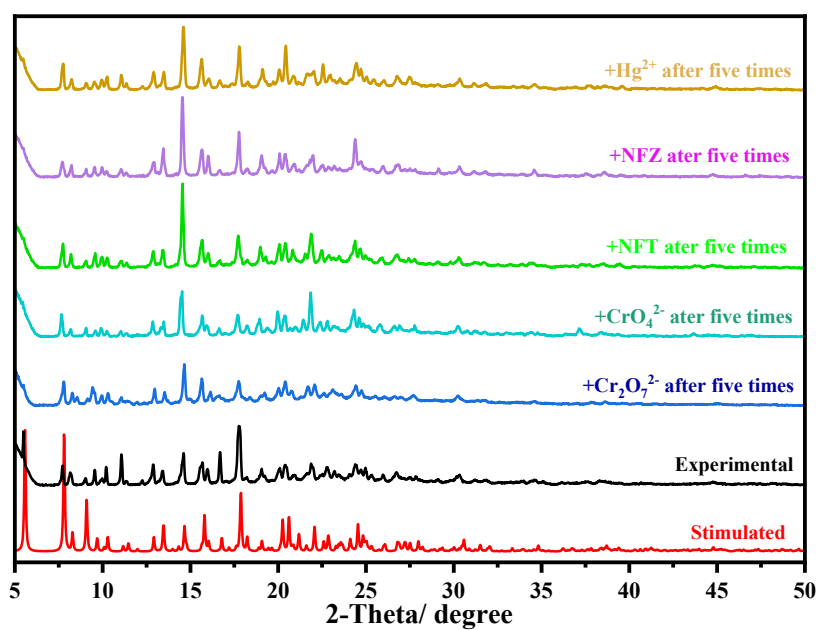

Fig. S5 The simulated and experimental PXRD patterns of **1** after sensing Hg^{2+}, $Cr_2O_7^{2-}$, CrO_4^{2-}, NFZ and NFT for 5 cycles
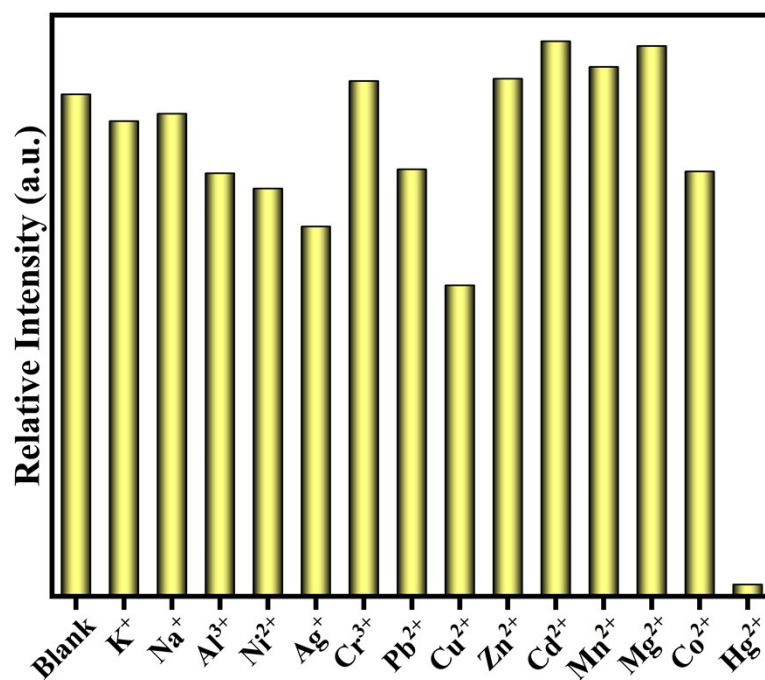
Fig. S6 Fluorescence Intensity of **1** in aqueous solution of different metal ion

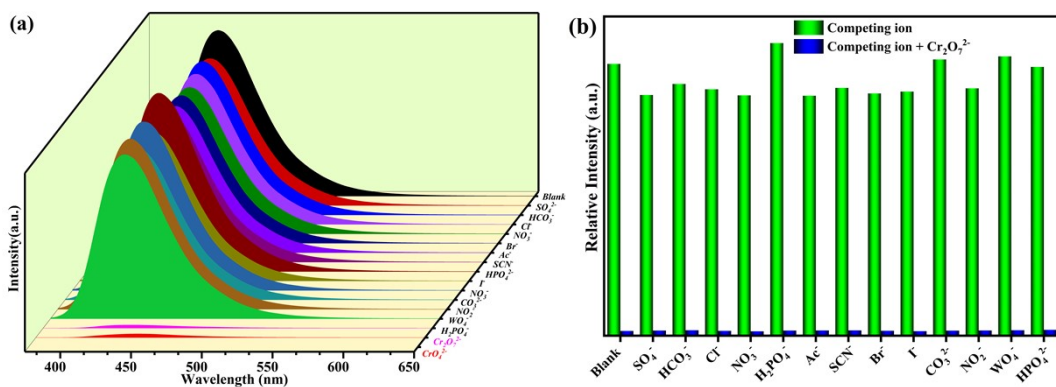**Fig. S7** (a) Fluorescence spectra of the suspension of **1** in different anions (b) Competitive experiments of **1** in sensing $Cr_2O_7^{2-}$ anion with the interference of other anion (0.5 mM) in H_2O solutions.
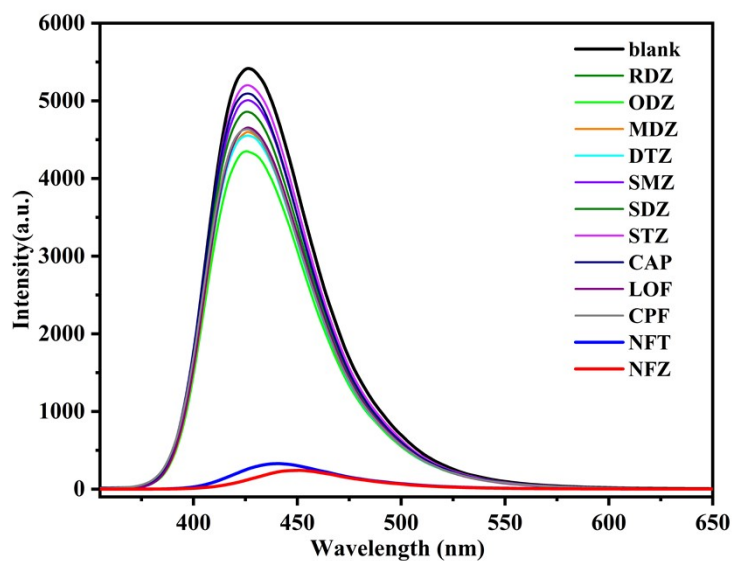
Fig. S8 Fluorescence spectra of the suspension of **1** in antibiotics compounds
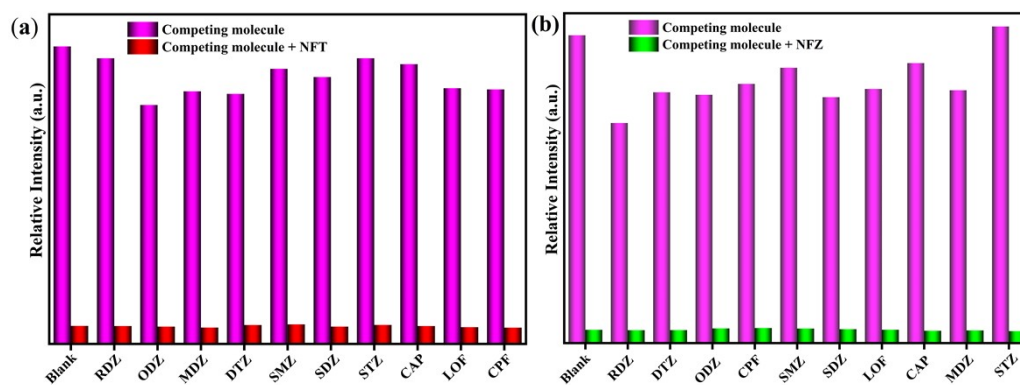
Fig. S9 Competitive experiments of **1** in sensing NFT (a) and NFZ (b) with the interference of other antibiotics compounds (0.2 mM) in H_2O solutions

Fig. S10 Luminescence response time of **1** after the addition of $Cr_2O_7^{2-}$ anion
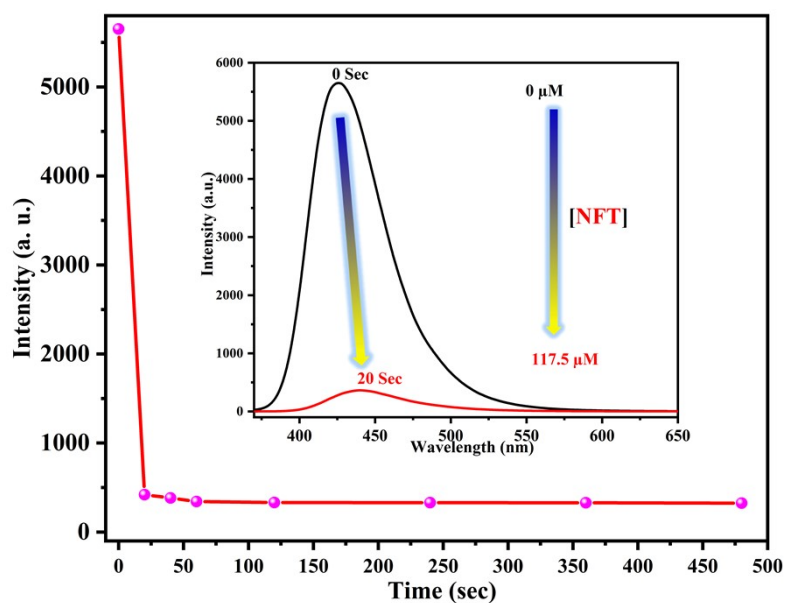
Fig. S11 Luminescence response time of **1** after the addition of NFT
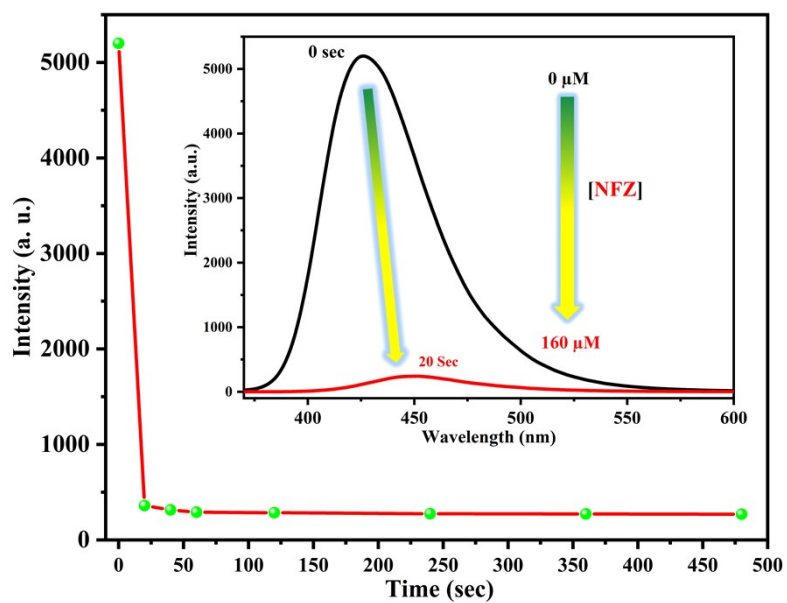
Fig. S12 Luminescence response time of **1** after the addition of NFZ
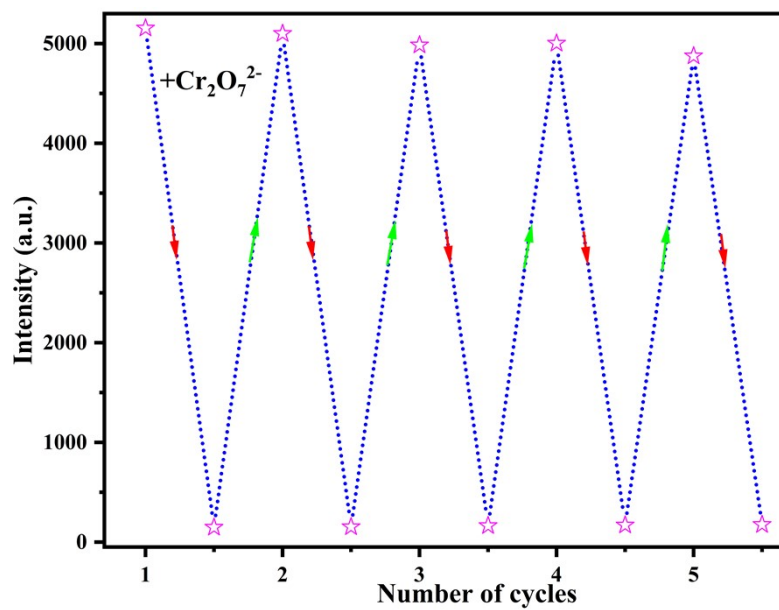
Fig. S13 Emission intensities of **1** toward $Cr_2O_7^{2-}$ after five cycles.
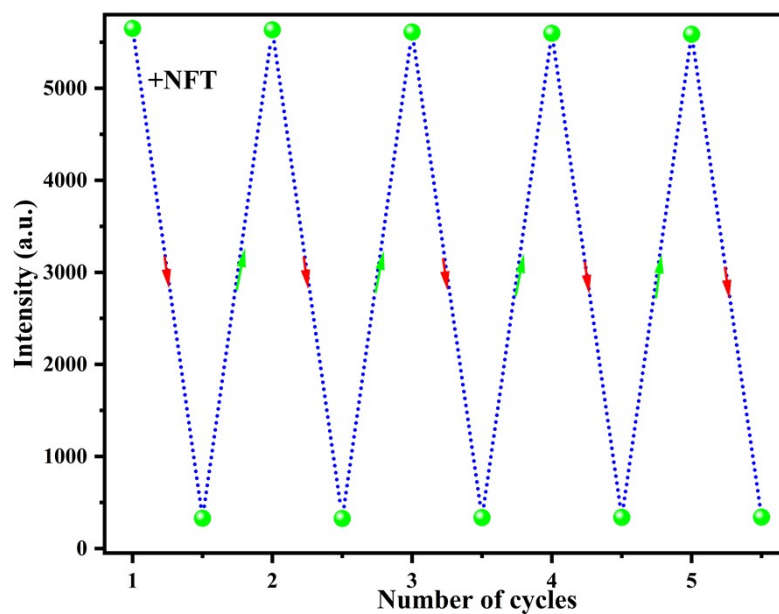
Fig. S14 Emission intensities of **1** toward NFT after five cycles.
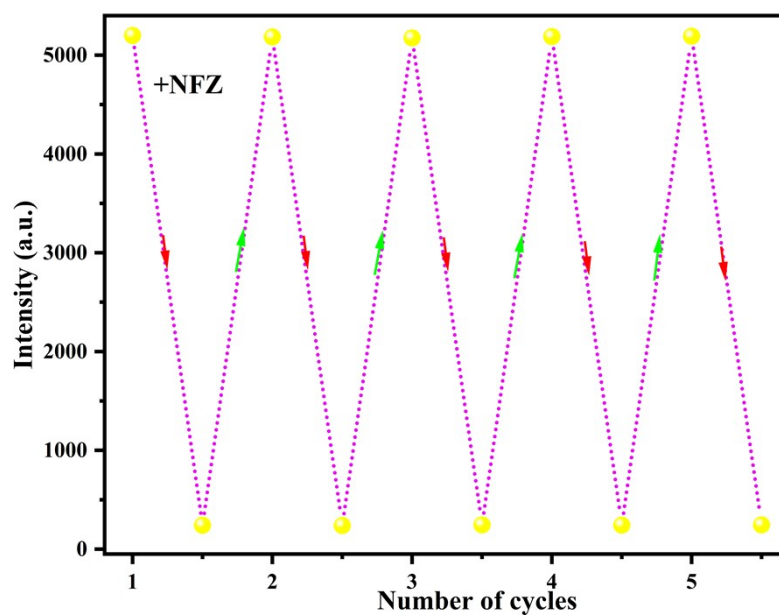
Fig. S15 Emission intensities of **1** toward NFZ after five cycles.
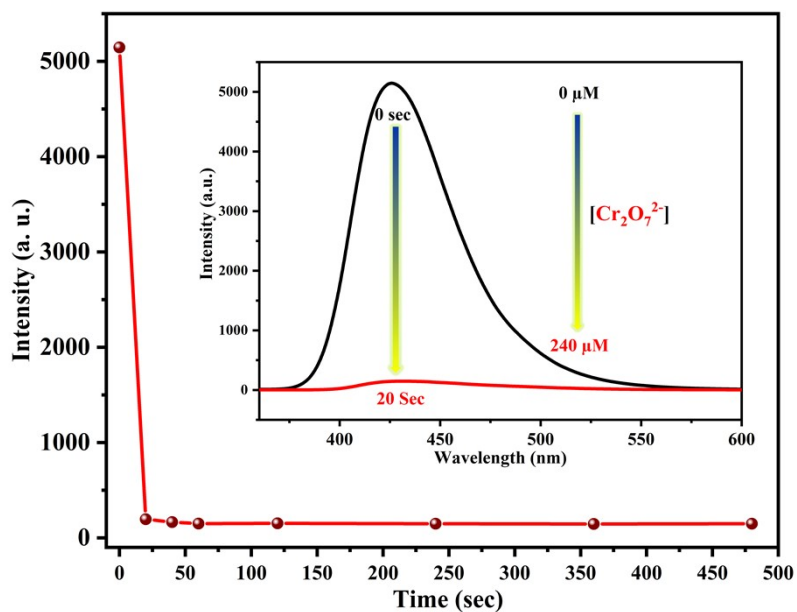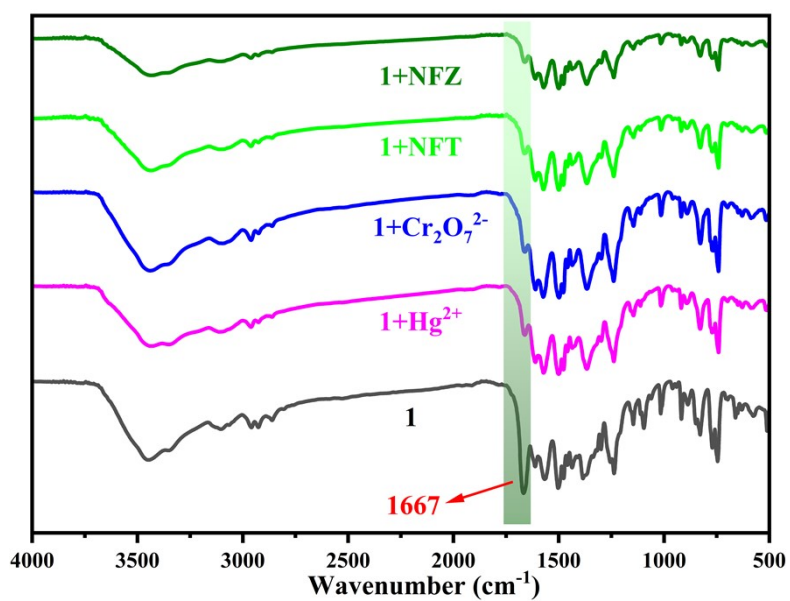

Fig. S16 IR spectra of **1** after sensing different analytes at room temperature. The intensity at the 1667 cm^{-1} absorption band reduced after being soaked in the H_2O solution, and the change in the IR spectra is due to the DMF molecules releasing from one dimensional (1D) channel.
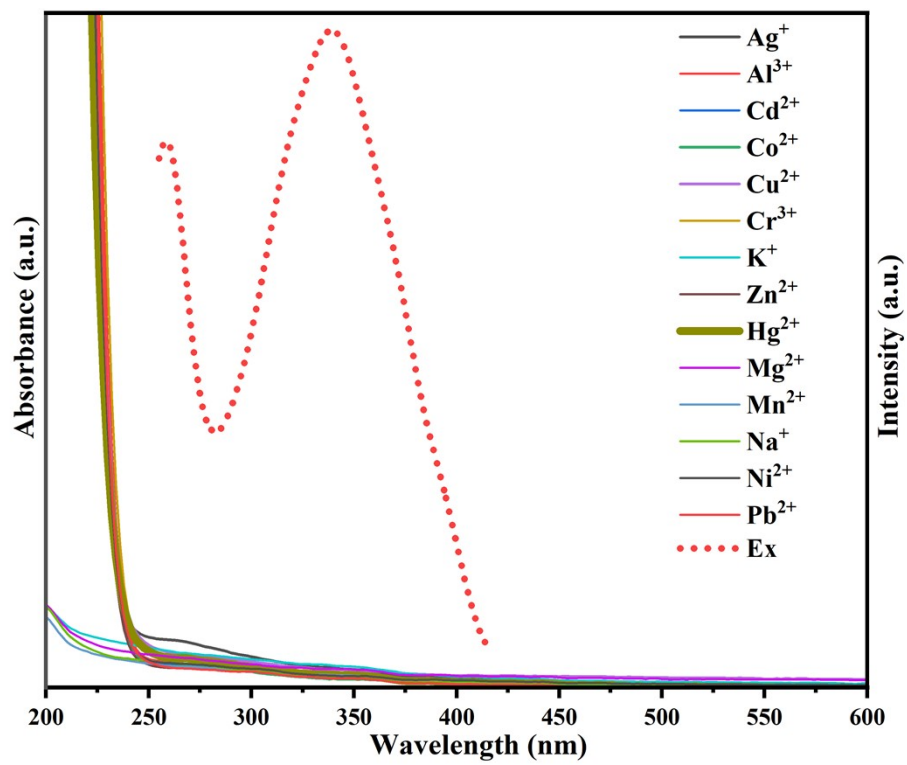
Fig. S17 The absorption spectra of cations and the excitation spectrum of **1**
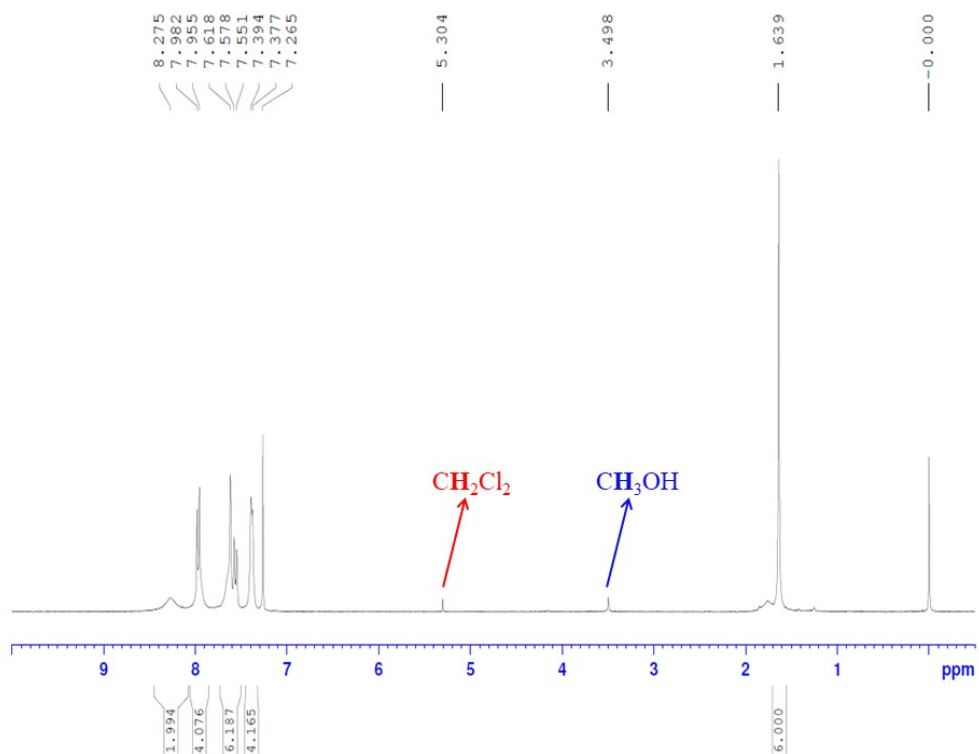
Fig. S18 ^{1}H NMR spectra of BBDF in CDCl$_3$
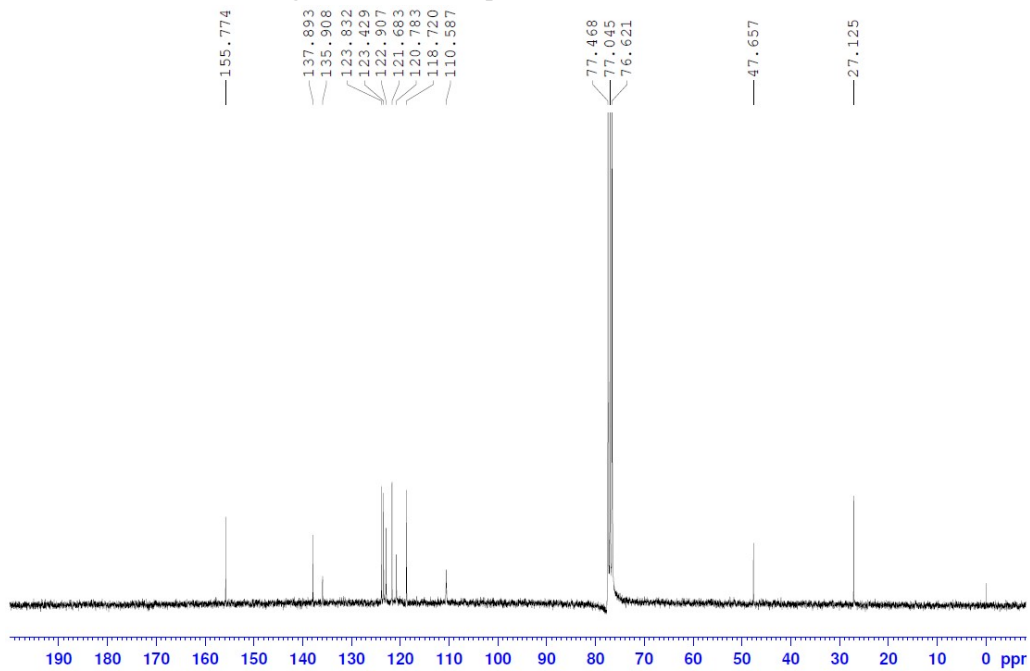
Fig. S19 ^{13}C NMR spectra of BBDF in CDCl$_3$

References

1. Rachuri, Y.; Parmar, B.; Bisht, K. K.; Suresh, E., Multiresponsive Adenine-Based Luminescent Zn(II) Coordination Polymer for Detection of Hg^{2+} and Trinitrophenol in Aqueous Media. *Crystal Growth & Design* **2017,** *17* (3), 1363-1372.

2. Xia, T.; Song, T.; Zhang, G.; Cui, Y.; Yang, Y.; Wang, Z.; Qian, G., A Terbium Metal-Organic Framework for Highly Selective and Sensitive Luminescence Sensing of Hg^{2+} Ions in Aqueous Solution. *Chemistry A European journal* **2016,** *22* (51), 18429-18434.

3. Manna, K.; Natarajan, S., Highly Selective MOF-Based Turn-Off Luminescence Detection of Hg^{2+} Ions in an Aqueous Medium and Its Dual Functional Catalytic Activity toward Aldol Condensation and beta-Enamination Reactions. *Inorg Chem* **2023,** *62* (1), 508-519.

4. Wu, P.; Liu, Y.; Liu, Y.; Wang, J.; Li, Y.; Liu, W.; Wang, J., Cadmium-Based Metal-Organic Framework as a Highly Selective and Sensitive Ratiometric Luminescent Sensor for Mercury(II). *Inorg Chem* **2015,** *54* (23), 11046-8.

5. Xiaoxiong, Z.; Wenjun, Z.; Cuiliu, L.; Xiaohong, Q.; Chengyu, Z., Eu^{3+}-Postdoped UIO-66-Type Metal-Organic Framework as a Luminescent Sensor for Hg^{2+} Detection in Aqueous Media. *Inorg Chem* **2019,** *58* (6), 3910-3915.

6. Wen, L.; Zheng, X.; Lv, K.; Wang, C.; Xu, X., Two Amino-Decorated Metal-Organic Frameworks for Highly Selective and Quantitatively Sensing of Hg(II) and Cr(VI) in Aqueous Solution. *Inorg Chem* **2015,** *54* (15), 7133-5.

7. Cao, X.-Q.; Wu, W.-P.; Li, Q.; Zheng, T.-F.; Chen, Y.-Q.; Chen, J.-L.; Liu, S.-J.; Wen, H.-R., Selective recognition of Hg^{2+} ions in aqueous solution by a Cd^{II}-based metal–organic framework with good stability and vacant coordination sites. *Dalton Transactions* **2023.** *52* (3), 652-658.

8. Ghosh, S.; Steinke, F.; Rana, A.; Biswas, S., A fluorescent zirconium organic framework displaying rapid and nanomolar level detection of Hg(ii) and nitroantibiotics. *Inorganic Chemistry Frontiers* **2022,** *9* (5), 859-869.

9. Xu, T. Y.; Nie, H. J.; Li, J. M.; Shi, Z. F., Highly selective sensing of Fe^{3+}/Hg^{2+} and proton conduction using two fluorescent Zn(ii) coordination polymers. *Dalton Trans* **2020,** *49* (32), 11129-11141.

10. Zhu, H.; Han, C.; Li, Y.-H.; Cui, G.-H., Two new coordination polymers containing long flexible bis(benzimidazole) ligand as luminescent chemosensors for acetylacetone and Hg(II) ions detection. *Journal of Solid State Chemistry* **2020,** *282.* 121132.

11. Wang, Z. J.; Ge, F. Y.; Sun, G. H.; Zheng, H. G., Two MOFs as dual-responsive photoluminescence sensors for metal and inorganic ion detection. *Dalton Trans* **2018,** *47* (25), 8257-8263.

12. Li, F.; Hong, Y.-S.; Zuo, K.-X.; Sun, Q.; Gao, E.-Q., Highly selective fluorescent probe for Hg^{2+} and MnO_4^- by the two-fold interpenetrating metal-organic framework with nitro functionalized linkers. *Journal of Solid State Chemistry* **2019,** *270*, 509-515.

13. Liu, W.; Qiao, J.; Gu, J.; Liu, Y., Hydrogen-Bond-Connected 2D Zn-LMOF with Fluorescent Sensing for Inorganic Pollutants and Nitro Aromatic Explosives in the Aqueous Phase. *Inorg Chem* **2023.** *62* (3), 1272-1278.

14. Xian, G.; Wang, L.; Wan, X.; Yan, H.; Cheng, J.; Chen, Y.; Lu, J.; Li, Y.; Li, D.; Dou, J.; Wang, S., Two Multiresponsive Luminescent Zn-MOFs for the Detection of Different

Chemicals in Simulated Urine and Antibiotics/Cations/Anions in Aqueous Media. *Inorg Chem* **2022,** *61* (19), 7238-7250.

15. Pal, S. C.; Mukherjee, D.; Das, M. C., pH-Stable Luminescent Metal-Organic Frameworks for the Selective Detection of Aqueous-Phase Fe(III) and Cr(VI) Ions. *Inorg Chem* **2022,** *61* (31), 12396-12405.

16. Chai, H. M.; Yan, J. L.; Zhang, G. Q.; Wang, J. X.; Ren, Y. X.; Gao, L. J., Five Mesoporous Lanthanide Metal-Organic Frameworks: Syntheses, Structures, and Fluorescence Sensing of Fe^{3+}, $Cr_2O_7^{2-}$, and H_2O_2 and Electrochemical Sensing of Trinitrophenol. *Inorg Chem* **2022,** *61* (19), 7286-7295.

17. Wang, T. T.; Liu, J. Y.; An, J. D.; Shi, Y. F.; Zhang, Y. Y.; Huo, J. Z.; Huang, Z. G.; Liu, Y. Y.; Ding, B., Hydrothermal synthesis of two-dimensional cadmium(II) micro-porous coordination material based on Bi-functional building block and its application in highly sensitive detection of Fe^{3+} and $Cr_2O_7^{2-}$. *Spectrochim Acta A Mol Biomol Spectrosc* **2021,** *254*, 119655.

18. Qin, B.; Zhang, X.; Qiu, J.; Gahungu, G.; Yuan, H.; Zhang, J., Water-Robust Zinc-Organic Framework with Mixed Nodes and Its Handy Mixed-Matrix Membrane for Highly Effective Luminescent Detection of Fe^{3+}, CrO_4^{2-}, and $Cr_2O_7^{2-}$ in Aqueous Solution. *Inorg Chem* **2021,** *60* (3), 1716-1725.

19. Gai, S.; Fan, R.; Zhang, J.; Sun, J.; Li, P.; Geng, Z.; Jiang, X.; Dong, Y.; Wang, J.; Yang, Y., Structural Design of Low Toxicity Metal-Organic Frameworks for Multifunction Detection of Organic and Inorganic Contaminants from Water. *Inorg Chem* **2021,** *60* (14), 10387-10397.

20. Fan, M.; Sun, B.; Li, X.; Pan, Q.; Sun, J.; Ma, P.; Su, Z., Highly Fluorescent Cadmium Based Metal-Organic Frameworks for Rapid Detection of Antibiotic Residues, Fe^{3+} and $Cr_2O_7^{2-}$ Ions. *Inorg Chem* **2021,** *60* (12), 9148-9156.

21. Sun, Q.; Yang, K.; Ma, W.; Zhang, L.; Yuan, G., A highly stable 8-hydroxyquinolinate-based metal–organic framework as a selective fluorescence sensor for Fe^{3+}, $Cr_2O_7^{2-}$ and nitroaromatic explosives. *Inorg Chem Front* **2020,** *7* (22), 4387-4395.

22. 1Singh, M.; Senthilkumar, S.; Rajput, S.; Neogi, S., Pore-Functionalized and Hydrolytically Robust Cd(II)-Metal-Organic Framework for Highly Selective, Multicyclic CO_2 Adsorption and Fast-Responsive Luminescent Monitoring of Fe(III) and Cr(VI) Ions with Notable Sensitivity and Reusability. *Inorg Chem* **2020,** *59* (5), 3012-3025.

23. Rath, B. B.; Vittal, J. J., Water Stable Zn(II) Metal-Organic Framework as a Selective and Sensitive Luminescent Probe for Fe(III) and Chromate Ions. *Inorg Chem* **2020,** *59* (13), 8818-8826..

24. Zhang, Y. Q.; Blatov, V. A.; Zheng, T. R.; Yang, C. H.; Qian, L. L.; Li, K.; Li, B. L.; Wu, B., A luminescent zinc(ii) coordination polymer with unusual (3,4,4)-coordinated self-catenated 3D network for selective detection of nitroaromatics and ferric and chromate ions: a versatile luminescent sensor. *Dalton Trans* **2018,** *47* (17), 6189-6198.

25. Xu, S.; Shi, J. J.; Ding, B.; Liu, Z. Y.; Wang, X. G.; Zhao, X. J.; Yang, E. C., A heterometallic sodium(i)-europium(iii)-organic layer exhibiting dual-responsive luminescent sensing for nitrofuran antibiotics, $Cr_2O_7^{2-}$ and MnO_4^{-} anions. *Dalton Trans* **2019,** *48* (5), 1823-1834.

26. Xu, Y.-L.; Liu, Y.; Liu, X.-H.; Zhao, Y.; Wang, P.; Wang, Z.-L.; Sun, W.-Y., Novel

cadmium(II) frameworks with mixed carboxylate and imidazole-containing ligands for selective detection of antibiotics. *Polyhedron* **2018,** *154,* 350-356.

27. Yang, H. W.; Xu, P.; Ding, B.; Liu, Z. Y.; Zhao, X. J.; Yang, E. C., A Highly Stable Luminescent Eu-MOF Exhibiting Efficient Response to Nitrofuran Antibiotics through the Inner Filter Effect and Photoinduced Electron Transfer. *European Journal of Inorganic Chemistry* **2019,** *2019* (48), 5077-5084.

28. Li, B.; Jiang, Y. Y.; Sun, Y. Y.; Wang, Y. J.; Han, M. L.; Wu, Y. P.; Ma, L. F.; Li, D. S., The highly selective detecting of antibiotics and support of noble metal catalysts by a multifunctional Eu-MOF. *Dalton Trans* **2020,** *49* (42), 14854-14862.

29. Wang, B.; Lv, X. L.; Feng, D.; Xie, L. H.; Zhang, J.; Li, M.; Xie, Y.; Li, J. R.; Zhou, H. C., Highly Stable Zr(IV)-Based Metal-Organic Frameworks for the Detection and Removal of Antibiotics and Organic Explosives in Water. *J Am Chem Soc* **2016,** *138* (19), 6204-6216.

30. Sun, S.-L.; Sun, X.-Y.; Sun, Q.; Gao, E.-Q., Highly efficient fluorescent chemosensor for nitro antibiotic detection based on luminescent coordination polymers with 2,6-di(4-carboxyphenyl)pyrazine. *CrystEngComm* **2021,** *23* (17), 3167-3174.

31. Fan, M.; Sun, B.; Li, X.; Pan, Q.; Sun, J.; Ma, P.; Su, Z., Highly Fluorescent Cadmium Based Metal-Organic Frameworks for Rapid Detection of Antibiotic Residues, Fe^{3+} and $Cr_2O_7^{2-}$ Ions. *Inorg Chem* **2021,** *60* (12), 9148-9156.

32. He, H.; Zhu, Q.-Q.; Li, C.-P.; Du, M. Design of a highly-stable pillar-layer zinc(II) porous framework for rapid, reversible, and multi-responsive luminescent sensor in water. *Crystal Growth & Design* **2019,** *19,* 694-703.

33. Zhai, Z.-W.; Yang, S.-H.; Cao, M.; Li, L.-K.; Du, C.-X.; Zang, S.-Q., Rational Design of Three Two-Fold Interpenetrated Metal–Organic Frameworks: Luminescent Zn/Cd-Metal–Organic Frameworks for Detection of 2,4,6-Trinitrophenol and Nitrofurazone in the Aqueous Phase. *Crystal Growth & Design* **2018,** *18* (11), 7173-7182.

34. Xu, N.; Zhang, Q.; Zhang, G., A carbazole-functionalized metal-organic framework for efficient detection of antibiotics, pesticides and nitroaromatic compounds. *Dalton Trans* **2019,** *48* (8), 2683-2691.

35. Zhang, Y. Q.; Wu, X. H.; Mao, S.; Tao, W. Q.; Li, Z., Highly luminescent sensing for nitrofurans and tetracyclines in water based on zeolitic imidazolate framework-8 incorporated with dyes. *Talanta* **2019,** *204,* 344-352.

36. Goswami, R.; Mandal, S. C.; Pathak, B.; Neogi, S., Guest-Induced Ultrasensitive Detection of Multiple Toxic Organics and Fe^{3+} Ions in a Strategically Designed and Regenerative Smart Fluorescent Metal-Organic Framework. *ACS Appl Mater Interfaces* **2019,** *11* (9), 9042-9053.

37. Liu, Y.; Zhang, Y.; Karmaker, P. G.; Tang, Y.; Zhang, L.; Huo, F.; Wang, Y.; Yang, X., Dual-Color 2D Lead-Organic Framework with Two-Fold Interlocking Structures for the Detection of Nitrofuran Antibiotics and 2,6-Dichloro-4-nitroaniline. *ACS Appl Mater Interfaces* **2022,** *14* (45), 51531-51544.

38. Li, Y. Z.; Wang, G. D.; Lu, Y. K.; Hou, L.; Wang, Y. Y.; Zhu, Z., A Multi-Functional In(III)-Organic Framework for Acetylene Separation, Carbon Dioxide Utilization, and Antibiotic Detection in Water. *Inorg Chem* **2020,** *59* (20), 15302-15311.

39. Xu, N.; Zhang, Q.; Hou, B.; Cheng, Q.; Zhang, G., A Novel Magnesium Metal-Organic Framework as a Multiresponsive Luminescent Sensor for Fe(III) Ions, Pesticides, and Antibiotics with High Selectivity and Sensitivity. *Inorg Chem* **2018,** *57* (21), 13330-13340.

40. Zhang, B.; Guo, P. Y.; Ma, L. N.; Liu, B.; Hou, L.; Wang, Y. Y., Two Robust In(III)-Based Metal-Organic Frameworks with Higher Gas Separation, Efficient Carbon Dioxide Conversion, and Rapid Detection of Antibiotics. *Inorg Chem* **2020,** *59* (7), 5231-5239.

41. Zhou, Z. H.; Dong, W. W.; Wu, Y. P.; Zhao, J.; Li, D. S.; Wu, T.; Bu, X. H., Ligand-Controlled Integration of Zn and Tb by Photoactive Terpyridyl-Functionalized Tricarboxylates as Highly Selective and Sensitive Sensors for Nitrofurans. *Inorg Chem* **2018,** *57* (7), 3833-3839.